

**GLOBAL JOURNAL OF ENGINEERING SCIENCE AND RESEARCHES**  
**INFLUENCE OF STRUCTURAL, ELECTRICAL AND MAGNETIC BEHAVIOUR OF**  
**SrAl<sub>2</sub>Fe<sub>12</sub>O<sub>22</sub> NANO SIZED POWDERS USING CHEMICAL CO-PRECIPIATION**  
**TECHNIC**

**Dr. M.N. Giriya<sup>1</sup>, Dr. C.L. Khobaragade<sup>2</sup>, Dr. K G Rewatkar<sup>3</sup>**

<sup>1</sup> Asso. Professor, Dept. of Appl. Physics, Smt. Radhikatai Pandav College of Engg. Nagpur, India

<sup>2</sup> Asst. Professor, Dept. of Appl. Physics, GovindraoWanjari College of Engg. & Technology,  
Nagpur, India.

<sup>3</sup> Asso.. Professor, Dept. of Physics, Dr Ambedkar College, Nagpur

---

**ABSTRACT**

In the present investigation, the samples with chemical composition SrAl<sub>2</sub>Fe<sub>12</sub>O<sub>22</sub> have been synthesized using perfect stoichiometric proportions of nitrates by chemical co-precipitation technique. The pellets of 15 mm diameter were prepared and sintered at 1100°C for 6 and 4 hrs and at 1000°C for 6 hrs separately. The characteristic studies have been done using XRD, SEM, electrical and magnetic properties. XRD studies of the samples showed hexagonal Y-type structure with unit cell dimensions ‘a’ and ‘c’ varies from a = 5 Å to 6 Å and c = 43 Å to 47 Å pertaining to space group P6<sub>3</sub>/mmc (No. 194). The variation in the values of lattice parameter has to be recorded with increase in Mn-Zn conc. The magnetic properties of prepared Y-type Ca-hexaferrite powder were investigated by VSM studies at 15,000 Gauss magnetic field. The transition temperature and activation energies have been investigated from electrical behaviour of the samples.

**Keywords:** XRD, SEM, VSM, Electrical and Magnetic Properties, Curie Temperature.

---

**I. INTRODUCTION**

Hexaferrites have been intensive studies due to a combination of good magnetic properties and low cost. This large family of oxides with hexagonal crystal structure contains ferrimagnetic compounds with easy axis of magnetization (e.g. M-type ferrites) and easy plane of magnetization (e.g. Y-type ferrites). Hence, hexaferrites have been widely adopted in two distinct fields: permanent magnets and microwave technology components [1]. On the other hand, Y-type ferrites SrAl<sub>2</sub>Fe<sub>12</sub>O<sub>22</sub> can undergo spin reorientation transitions (SRT) between different anisotropy configurations (easy plane easy cone/easy axis) induced by change of temperature or applied magnetic field [2-9]. The transition temperature can be tuned by modifying the chemical composition (substitution of divalent and trivalent metal ions). Moreover, some potential application of Y-type hexaferrites at 1100°C & 1000°C temperatures have been such as magnetic recording media, permanent magnets, magnetic yokes, latches, phase shifter etc [6, 7].

Conventional ceramic method of hexaferrite synthesis is efficient, but requires elevated temperatures for solid state reaction to occur between premixed powders. Alternative production routes (aerosol pyrolysis, chemical co-precipitation, glass crystallization, hydrothermal synthesis, etc.) are intended to improve mixing of initial components down to atomic level and thereby to facilitate diffusion. In particular, a chemical co-precipitation technique enables to obtain sufficiently homogeneous precursors for low temperature synthesis of nanosized ferrites. However, hexagonal ferrites with complex layered crystal structures still require relatively high temperatures to form because of thermodynamic stability conditions. Trying to avoid rapid growth of grains, we have used this soft-chemistry approach for production of Y-type ferrites. An important goal was to determine the heat treatment regimes ensuring complete transformation of a precursor into the smallest particles of single Y-phase. In this paper the results of structural, electrical, magnetic and mechanical characterization SrAl<sub>2</sub>Fe<sub>12</sub>O<sub>22</sub> of powders are presented.

## II. MATERIALS AND METHODS

Hexaferrite powders have been prepared by a chemical co-precipitation method [10]. The A. R. grade nitrates have been used as starting material. Stoichiometric proportion of strontium nitrate, ferric nitrate, aluminium nitrate (99.9%) etc. have been dissolved one by one in 100 ml of de-ionized water. Ammonia solutions (30%) have been added slowly in the mixture to adjust pH of 8. The mixed solutions have been stirred for 2 hr and will be kept at room temperature for 24 hr for aging. The calcium hexaferrites precipitates have been separated in a centrifuge machine at 2500 rpm for 20 minute. The prepared precipitates have been washed in 1:1 mixture of methanol and acetone followed by 100% de-ionized water to remove impurities. The precipitates have been dried at 100°C for 24 hrs and calcinated at 1000°C & 1100°C for 4 hrs and 6 hrs separately to obtain SrAl<sub>2</sub>Fe<sub>12</sub>O<sub>22</sub> hexaferrite particles [11].

Crystal structure has been examined by PA Analytical X'Pert Pro X-ray diffraction (XRD) in Cu-K $\alpha$  radiation with accelerator detector for rapid data acquisition. To ensure the single phase formation of the hexagonal structure, X-ray studies have been carried out. Magnetization curves were recorded on Lake Shore vibrating sample magnetometer (VSM). The lattice parameters and X-ray densities of the samples have been computed from XRD analysis. The bulk density has been determined by mass and bulk volume of the samples, while porosity for each sample has been calculated separately. Structural analysis has been carried out from SEM and XRD of the studied materials.

## III. RESULTS

### Structural analysis

The Sr-Y hexaferrites (SrAl<sub>2</sub>Fe<sub>12</sub>O<sub>22</sub>) with substitution of aluminium(Al) calcinated at temperatures at 1100°C for 6 and 4 hrs and at 1000°C for 6 hrs separately. The crystallographic results described (Table-1) and the XRD pattern (Figure 1) reveals the hexagonal crystal structure and most of the lines can unequivocally be indexed for the magnetoplumbite structure. All the three members of series with the values 'a' and 'c' and cell volume varies in the range of a = 5.84Å to 5.87Å and c = 44.02Å to 44.44Å and cell volume V = 1300.762Å<sup>3</sup> to 1330.189 Å<sup>3</sup> (Table-1). However these values are analogous to the values a = 5.69Å and c = 45.2906Å for Sr<sub>2</sub>Cu<sub>2</sub>Fe<sub>12</sub>O<sub>22</sub> calcinated at 950°C for 4 hours as mentioned in Jotaniaet *at el* (2012) [15]. This variation in the value of 'a' and 'c' is obvious as ionic radii of Al<sup>3+</sup>(0.535Å) is smaller as compared to Sr<sup>2+</sup>(1.18Å) than Fe<sup>3+</sup>(0.645Å) ions which has replaced Fe<sup>3+</sup> ions i.e. atoms shrinks towards a and c axis.

From the SEM photograph (Figure 2(a), 2(b), 2(c)), the average grain size of SrAl<sub>2</sub>-Y ferrites is geometrically estimated. The particle size varies in the range of 70 nm to 50 nm for the calcinations temperature from 1100°C to 1000°C for time interval of 6 hours and 70 nm to 35nm for the calcinations temperature of 1100°C for time interval of 6 to 4 hours. It means that the sizes of the molecules of the samples are observed in nano range which are hexagonal in shape and also it is concluded from the calculated values of XRD analysis [12, 13].

The bulk density of the compounds of these series is observed to be decreased with the decreasing calcinations temperature from 1100°C to 1000°C for time interval of 6 hours and also for the calcinations temperature of 1100°C for time interval of 6 to 4 hours, which may be due to contraction of grain size due to decrease of the calcinations temperature with time. The X-ray density (d<sub>x</sub>) are calculated, which depends on the molecular weight and the volume of the samples. The bulk density (d<sub>b</sub>) of the sample has been calculated from the geometry and the mass of the samples. The percentage porosity (P) of the samples has been calculated from X-ray density and bulk density, which shows rising trend with decreasing calcinations temperature (Table-1).

The X-ray density has been calculated using the relation for hexagonal ferrite [13] given below:

$$dx = \frac{2M}{N \cdot 0.866a^2c}$$

where, M = molecular weight of the sample, volume (V) for hexagonal =  $0.866a^2c$ , N =

Avogadro's number & Lattice parameters is a, c.

The X-ray density (dx) depends on the lattice constant and molecular weight of the samples whereas the bulk density ( $d_B$ ) of the sample can be calculated from the geometry of the crystals and mass of the samples.

The well-known Scherrer formula has been used to determine the particle size from the line broadening of diffraction profile of the strongest peak. The formula, excluding the effects of the machine broadening to minimize errors, is given below:

$$D = \frac{k\lambda}{b \cos \theta}$$

where, D = average particle size, k = Scherrer constant (k = 0.9),  $\lambda$  = wavelength of radiation (1.54056 Å), b = peak width at half height [full width half maxima (FWHM)] and  $\theta$  corresponds to the peak position measured in radians. It shows that the particle size varies in the range from 72.26 nm to 59.13 nm. It means that the size of the particle is very small and they are closely bound with each other in the crystal structure. Therefore less porosity is found in these compounds.

In order to monitor the structural changes during the synthesis process, FTIR spectra of dried compounds of this series have been taken within wave number range from  $4000\text{cm}^{-1}$  to  $400\text{cm}^{-1}$  (Figure 3(a), 3(b), 3(c)). The spectra of dried compounds for  $\text{SrAl}_2\text{Y}$ -hexaferrites has been shown in (Table-2), indicates the characteristics bands in the range  $455.20\text{ cm}^{-1}$  to  $563.21\text{ cm}^{-1}$  which attributes to Sr-O-Al stretching vibration of the  $\text{SrAl}_2\text{-Y}$  hexaferrites by Jotania *et al* (2012) [15].

### Electrical properties

The electrical studies of the samples under study were measured by applying dc voltage. The electrical conductivity and dielectric measurement are done by two probe method in the temperature range 303 K to 703 K. The plot of logarithmic electric conductivity versus inverse of temperature shows changes in slope in the neighborhood of Curie temperature ( $T_c$ ). The activation energy below and above the Curie temperature was calculated separately. It has been observed that the activation energy is less in ferrimagnetic and more in paramagnetic region, which indicates semiconducting nature of the compounds [16].

The electrical resistivity-temperature behaviour of the sample obeys the Willson's law

$$\rho = \rho_0 \exp\left(\frac{\Delta E}{KT}\right)$$

It has been seen from the (Figure 4(a), 4(b), 4(c)) that the transition temperature ( $T_1$ ) at which the kinks in the plot of  $\log(\sigma)$  versus  $1/T$  was observed in the specimens under investigations is in the neighborhood of its Curie temperature ( $T_c$ ). This reveal that the kinks observed in Aluminium substituted Sr-Y ferrites have been attributed to the magnetic transition. A minute change in slope of Curie temperature in the plot of  $\log(\rho)$  Vs  $10^3/T$  for  $\text{Sr}_2\text{Ni}_2\text{Fe}_{12}\text{O}_{22}$  was observed by Asmat Elahi *et al* (2013) [17]. The electrical conductivity results obtained at room temperature are given in (Table-3) and logarithmic conductivity ( $\log\sigma$ ) versus inverse of temperature ( $1/T$ ) plots has been shown in (Figure 4(a), 4(b), 4(c)). It is evident that the value of electrical conductivity at room temperature varies in the ranges of  $0.193 \times 10^{-4}$  to  $0.389 \times 10^{-4} \Omega^{-1}\text{cm}^{-1}$ .

The dielectric measurements have been carried out over the frequency range 100Hz to 9.9MHz at room temperature using Weyn Kerr precision impedance Analyser 6500B. The variation of dielectric loss tangent  $\tan(\delta)$  with the log

(F) for the series of compounds (Figure 5(a), 5(b), 5(c)). It clears from the figure that the dielectric loss tangent ( $\tan\delta$ ) decreases with the increasing measuring frequency.

### Magnetic properties

The B-H curve measurement have been carried out in the compounds which are calcinated at 1100°C and 1000°C for 6 hours in order to study its coercivity, remanance, saturation magnetization and squareness ratio from these values magnetic moments were calculated.

The hysteresis loops have been traced at varying external applied magnetic field of 15000 G, volume of the sample has been taken about 24 to 41 mg. The shape and size of hysteresis loop obtained for these two compounds (Figure 6(a), 6(b)). If we compare the size and shape of compounds, it has been observed that Sr-Y hexaferrites calcinated at 1100°C for 6 hours is more magnetic in nature than Sr-Y hexaferrites calcinated at 1000°C for 6 hours. The above observation is corroborated with the evidence showing larger value of coercivity, remanance, and saturation magnetization for Sr-Y hexaferrites calcinated at 1100°C for 6 hours. It has been observed from the result that for Sr-Y hexaferrite saturation magnetization( $M_s$ ), remanance( $M_r$ ) and coercivity ( $H_c$ ) decrease as calcinations temperature decreases from 1100°C to 1000°C for the time interval of 6 hours. Same trend is observed in other hexaferrites, calcinated at different higher temperatures for  $Sr_2Ni_2Fe_{12}O_{22}$ .as reported in Asmat Elahi *et al* (2013) [15]. As hysteresis study has been carried out at the external magnetic field of 15000 G, the compounds showing a nature of soft ferrites however at higher magnetic field, it has been showing higher values of coercivity, remanance and saturation magnetization.

## IV. DISCUSSION

The variation in the value of ‘a’ and ‘c’ is obvious as ionic radii of  $Al^{3+}(0.535\text{Å})$  is smaller as compared to  $Sr^{2+}(1.18\text{Å})$  than  $Fe^{3+}(0.645\text{Å})$  ions which has replaced  $Fe^{3+}$  ions i.e. atoms shrinks towards a and c axis. It is also found that, almost all the reflection of the reported compounds has been indexed in our compounds. The exact matching of crystallographic data of the above sample to that of reported one confirms the formation of all the samples in a single homogeneous phase with hexagonal structure [8]. It has been observed that there were no significant changes in the crystal lattice of Aluminium substituted Sr-Y hexaferrites found with changing calcinations temperature from 1100°C to 1000°C within time interval of 6 hours to 4 hours.

These strontium ions with ionic radius ( $1.18\text{Å}$ ) are slight smaller than the oxygen ions with ionic radius ( $1.4\text{Å}$ ). Therefore the distance between the oxygen layers which contain no strontium ion are  $2.41\text{Å}$  and  $2.35\text{Å}$  respectively. The projection of the distance between the centers of the Sr ions on to the axis is  $2.58\text{Å}$ , from which it follows that the centers of the strontium ions lies at a distance of  $0.17\text{Å}$  out of the plane of the nearest oxygen layer [17].

The SEM results reveal that the grain size varies in the range of 70 nm to 50 nm for the calcinations temperature from 1100°C to 1000°C for time interval of 6 hours and 70 nm to 35nm for the calcinations temperature of 1100°C for time interval of 6 to 4 hours. It means that the sizes of the molecules of the samples are observed in nano range which are hexagonal in shape and also it is concluded from the calculated values of XRD analysis [12, 13].

The bulk density of the compounds of these series is observed to be decreased with the decreasing calcinations temperature from 1100°C to 1000°C for time interval of 6 hours and also for the calcinations temperature of 1100°C for time interval of 6 to 4 hours, which may be due to contraction of grain size due to decrease of the calcinations temperature with time. Other reason might be the modification may be due to difference in the specific gravity of compositional oxides that may be affected with changing calcinations temperature.

The X-ray density ( $d_x$ ) depends on the molecular weight and the volume of the samples. The bulk density ( $d_B$ ) of the sample has been calculated from the geometry and the mass of the samples. The percentage porosity (P) of the samples has been calculated from X-ray density and bulk density, which shows rising trend with decreasing calcinations temperature. This is due to the fact that value of lattice parameter gets altered by decreasing the calcinations temperature which leads to increase the porosity for Sr-Y hexaferrites. In this context another reason might be difference in the melting point of the reacting oxides used. The numbers of the pores get reduced at higher temperature at 1100 °C as a result of which the individual grains come closer to each other and effective cross sectional area of grains to grains contact increases. This in turn results in greater densification and less porosity at higher temperature [14].

The particle size of the studied compound varies in the range from 70 nm to 50 nm (Table 1). It means that the size of the particle is very small and they are closely bound with each other in the crystal structure. Therefore less porosity is found in these compounds.

The FTIR spectra of dried compounds of this series are taken within wave number range from 4000 $\text{cm}^{-1}$  to 400 $\text{cm}^{-1}$ . The spectra of dried compounds for SrAl<sub>2</sub>Y-Hexaferrites indicates the characteristics bands in the range 455.20  $\text{cm}^{-1}$  to 563.21  $\text{cm}^{-1}$  which attributes to Sr-O-Al stretching vibration of the SrAl<sub>2</sub>-Y hexaferrites by Jotania *et al* (2012) [15].

The plot of logarithmic electric conductivity versus inverse of temperature shows changes in slope in the neighborhood of Curie temperature ( $T_c$ ). The activation energy below and above the Curie temperature has been calculated separately. It has been observed that the activation energy is less in ferrimagnetic and more in paramagnetic region. The plots are linear indicating any absence of impurity in crystal lattice. An increase of the temperature from room temperature, the resistivity of the sample decreases for each of compound in the Sr-Y series of the hexaferrites, which attributes directly about the tight bonding of ions at room temperature at their interstitial sites, which originates the hopping mechanism in the crystal lattice. The activation energy was found to be decreasing with the decreasing calcinations temperature. The conduction mechanism may be explained on the basis of Koop's hopping mechanism of the localized d-electron model for Y-Type hexaferrites [18].

This decrease behaviour of dielectric loss tangent ( $\tan \delta$ ) with the increasing frequency has been explained on the basis of the assumption that is made in the mechanism of polarization process in ferrites. The behaviour of  $\tan \delta$  with the frequency shows relaxation peaks which shift towards lower frequencies with decreasing calcinations temperature from 1100 °C to 1000 °C [19].

It has been observed from the result that for Sr-Y hexaferrite saturation magnetization ( $M_s$ ) increase but remanance ( $M_r$ ) decreases, as calcinations temperature decreases from 1100 °C to 1000 °C. These modifications in the values has been observed due to Fe-O-Fe exchange interaction and reduced in lattice dimension site which directly affects on site distribution, Curie constant and saturation magnetization. The temperature dependence of magnetization can be explain in light of cationic distribution and lattice dislocation among the available tetrahedral and octahedral sites in spinal and garnet site [20].

## V. CONCLUSION

Y-type barium hexaferrite have been synthesized by chemical co-precipitation method using nitrates. The obtained products exhibit well crystalline phase of SrAl<sub>2</sub>Fe<sub>12</sub>O<sub>22</sub> typical hexagonal structure. The magnetic measurement for the calcined Y-type hexaferrite was observed and the values are compared with previous research reports, which exhibits enhanced hard magnetic property due to the reduced particle size. The electrical conductivity measurements observed Curie temperature in the range 423K to 498K. The activation energies have been found in the range of 0.261 eV to 0.349 eV in ferrimagnetic and 0.386 eV to 0.611 eV in paramagnetic region.

## VI. SUMMARY OF RESEARCH

1. The lattice parameter 'a' shows the decreasing trend and 'c' values shows increasing trend with the added impurities this is due to the difference between ionic radii of  $Al^{3+}$  (0.535 Å) is smaller as compared to  $Si^{2+}$  (1.18 Å) than  $Fe^{3+}$  (0.645 Å) ions which has replaced  $Fe^{3+}$  ions i.e. atoms shrinks towards a and c axis.
2. The particle size for the studied samples have been calculated and found in the range of 72.26 nm to 59.13 shown in (Table 1). It has been reported that the crystallite size less than 50 nm is required in obtaining the suitable signal-to-noise ratio in the high density recording media.
3. The Curie temperature ( $T_c$ ) has been found in the range of 423K to 498 K. The activation energy has been found in the range of 0.261 eV to 0.349 eV in ferrimagnetic and 0.386 eV to 0.611 eV in paramagnetic region.
4. The saturation magnetization carried out 0.35683 emu/g at 1100 °C &  $8.5899 \times 10^{-3}$  emu/g at 1000 °C, coercivity is 8017.7 G at 1100 °C & 2401.3 G at 1000 °C, remanance of magnetization is 0.2124 emu/g at 1100 °C &  $1.82 \times 10^{-3}$  emu/g, squareness ratio ( $M_r/M_s$ ) is 0.5953 at 1100 °C & 0.2110 at 1000 °C.
5. It is well known that the coercivity of barium hexaferrite depends on many factors, such as chemical composition, particle size, degree of crystallinity, microstructure, magnetic anisotropy, etc.

## VII. FUTURE ISSUES

I believe that many scientists doing work on Y-type ferrite. To pay attention to the real research on ferrite data obtained from last 20 years and summarized a little in this work. The main application of this developed material is in high density recording media in obtaining suitable signal-to-noise ratio.

## VIII. DISCLOSURE STATEMENT

There is no special financial support for this research work from the funding agency.

## IX. ACKNOWLEDGEMENT

I expressed big gratitude to the Dr. K. G. Rewatkar whose continue support for the research activities. These works initiated systematic research of any problem and receiving many new results in this area. It is a lot of thanks to my colleagues for constructive support.

## REFERENCES

1. Raj K, Moskowitz R and Casciari R, *J. Magn. Magn. Mater.*, 1995, 149, 174.
2. Vishwanathan B, Moorthy V R K, *Ferrite Materials: Science and Technology*, Springer Verlag, 1990.
3. Verwey E.J.W. and De Boer J.H., *Rec. Trans. Chem. Des. Pays. Bas.* 1936, 55, 531.
4. Koops C.G., "On the dispersion of Resistivity and Dielectric Constant of Some Semiconductor at Audio Frequency", *Physical Review*, 1951, 83, 121.
5. Subramanian A., Marks L.D., *Ultramicroscopy*, 2004, 98, 1-5.
6. Smith D.R., Morgan R.L., Loewenstein E.V. "Comparison of the Radiance of Far-Infrared Sources". *J. Opt. Soc. Am.* 1968, 58 (3), 433-434.
7. Mukhtar Ahmad, Ihsan Ali, Islam M.U., and Rana M.U., *Journal of Materials Engineering and Performance*, ISSN 1059-9495, 2013, DOI 10.1007/s11665-013-0662-4.
8. Cullity B.D., "Elements of X-Ray Diffraction," Addison-Wesley Publishing, Boston, 1976.
9. Kamba S., Goian V., Savinov M., *Comparison of ceramics and single crystals: Journal of Applied Physics*, 2010, 107, 10.
10. Satone B. S., Kakde A. S., Gothe M. J., Rewatkar K. G., Sawadh P. S., *Int. J. Res. in Biosciences, Agriculture and Tech.* ", Issue 2, 2014, 1, 949 - 955.
11. Jotania R. B., Khomane R. B., Deshpande A. S., Chauhan C. C., Kulkarni B. D., *J Sci. Res.I*, 2009, 1, 1-13

12. Kumar S., Kumar G. and Singh M., *J. IntegrSciTechnol*, 2015, 1(3), 1-5.
13. J. Wang, P. F.Chong, S. C. Ng and L. M. Gan, "Microemulsion processing of manganese zinc ferrites", *Materials Letters, Issue2-3(30)*, pp 217-221(1997).
14. Moinuddin M.K. and Murthy S.R., *J. Alloys Compound*, 1993, 194, 105.
15. Rajshree B. Jotania, Pratiksha A. Patel, *International Journal of Engineering Research and Applications (IJERA)*, Vol. 2, Issue 4, pp.494-498 (2012).
16. Mukhtar Ahmad, Qasim Ali, Ihsan Ali, Ishtiaq Ahmad, *Journal of Alloys and Compounds*, 2013, 580, 23–28.
17. Asmat Elahi, Mukhtar Ahmad, *Ceramics International*, 39, 983–990 (2013).
18. Koops C.G., *Phys. Rev. USA*, 1951, 83[1], 121-124.
19. Nandotaria Reshma A., Jotania Rajshree B., *International Journal of Soft Computing and Engineering*, 2011, 1(1), 45-48.
20. Sharma P.U, Raval J.V, Zankat K.B, Dolia S.N, 53<sup>rd</sup> DAE Solid State Physics Symposium, BARC & TIFR, Mumbai, 2008, 16-20.

**TABLES:**

| Table-1<br>Sr-Y hexaferrite calcinated at different temp. for 4 and 6 hours showing lattice constants, particle size, bulk density, X-ray density, porosity, molecular wt and Curie temp. |                       |            |                  |       |     |                           |                      |  |   |                     |                        |                                   |
|---|-----------------------|------------|------------------|-------|-----|---------------------------|----------------------|--|---|---------------------|------------------------|-----------------------------------|
| Sample  | Calcination Temp (°C) | Time (Hrs) | Lattice Constant |       |     | Volume V(Å <sup>3</sup> ) | Particle size S (nm) | Bulk density $d_B$ (gm/cm <sup>3</sup> ) | X-ray Density $d_x$ (gm/cm <sup>3</sup> ) | Porosity (Fraction) | Molecular wt (gm/mole) | Curie Temp. (T <sub>c</sub> ) (K) |
|   |                       |            | a (Å)            | c (Å) | c/a |                           |                      |  |   |                     |                        |                                   |
| SrAl <sub>2</sub> Fe <sub>12</sub>  | 1100                  | 6          | 5.88             | 44.   | 7.5 | 1313.8                    | 72.26                | 2.286                                    | 4.456                                     | 0.48                | 1163.7                 | 463                               |
| SrAl <sub>2</sub> Fe <sub>12</sub>  | 1100                  | 4          | 5.88             | 44.   | 7.5 | 1330.1                    | 36.09                | 2.077                                    | 4.  | 0.52                | 1163.7                 | 423                               |
| SrAl <sub>2</sub> Fe <sub>12</sub>  | 1000                  | 6          | 5.84             | 44.   | 7.5 | 1300.7                    | 59.13                | 2.018                                    | 4.357                                     | 0.53                | 1163.7                 | 498                               |

| Table-2<br>Sr-Y hexaferrite sample shows absorption peaks of FTIR spectra. |                       |            |                             |                             |
|--|-----------------------|------------|-----------------------------|-----------------------------|
| Sample   | Calcination Temp (°C) | Time (Hrs) | Absorption Peaks            |                             |
|  |                       |            | Upper peak cm <sup>-1</sup> | Lower peak cm <sup>-1</sup> |
| SrAl <sub>2</sub> Fe <sub>12</sub> O <sub>22</sub>                         | 1100                  | 6          | 563.21                      | 464.84                      |
| SrAl <sub>2</sub> Fe <sub>12</sub> O <sub>22</sub>                         | 1100                  | 4          | 561.29                      | 455.20                      |
| SrAl <sub>2</sub> Fe <sub>12</sub> O <sub>22</sub>                         | 1000                  | 6          | 555.50                      | 491.85                      |

| Table 3<br>Sr-Y hexaferrite compounds shows conductivity and activation energies in ferri an para magnetic region. |  |
|--|--|
|  |  |

| Sample   | Calcination Temp (°C) | Time (Hrs) | Room temp. Resistivity( $\rho$ ) ( $\Omega$ .cm) | Room temp. Conductivity( $\sigma$ ) ( $\Omega$ .cm) <sup>-1</sup> | Activation Energy $\Delta E$ |           |
|--|-----------------------|------------|--|---|------------------------------|-----------|
|  |                       |            |  |   | Ferri (eV)                   | Para (eV) |
| SrAl <sub>2</sub> Fe <sub>12</sub> O <sub>22</sub> | 1100                  | 6          | 4.1 x10 <sup>4</sup>                             | 0.243x10 <sup>-4</sup>  | 0.297                        | 0.454     |
| SrAl <sub>2</sub> Fe <sub>12</sub> O <sub>22</sub> | 1100                  | 4          | 5.16 x10 <sup>4</sup>                            | 0.193x10 <sup>-4</sup>  | 0.261                        | 0.386     |
| SrAl <sub>2</sub> Fe <sub>12</sub> O <sub>22</sub> | 1000                  | 6          | 2.57 x10 <sup>4</sup>                            | 0.389x10 <sup>-4</sup>  | 0.349                        | 0.611     |

Table 4  
The Sr-Y hexaferrite sample shows coercivity, remanance, saturation magnetization and squareness ratio from VSM of each sample.

| Sample   | Calcination Temp (°C) | Time (Hrs) | Coercivity (H <sub>c</sub> ) (Gauss) | Remanance (M <sub>r</sub> ) (emu/gm) | Saturation Magnetization (M <sub>s</sub> ) (emu/ gm) | Squareness Ratio M <sub>r</sub> /M <sub>s</sub> |
|--|-----------------------|------------|--------------------------------------|--------------------------------------|--|---|
| SrAl <sub>2</sub> Fe <sub>12</sub> O <sub>22</sub> | 1100                  | 6          | 8017.7                               | 0.2124                               | 0.35683  | 0.5953  |
| SrAl <sub>2</sub> Fe <sub>12</sub> O <sub>22</sub> | 1000                  | 6          | 2401.3                               | 1.82x10 <sup>-3</sup>                | 8.5899x10 <sup>-3</sup>                              | 0.2110  |

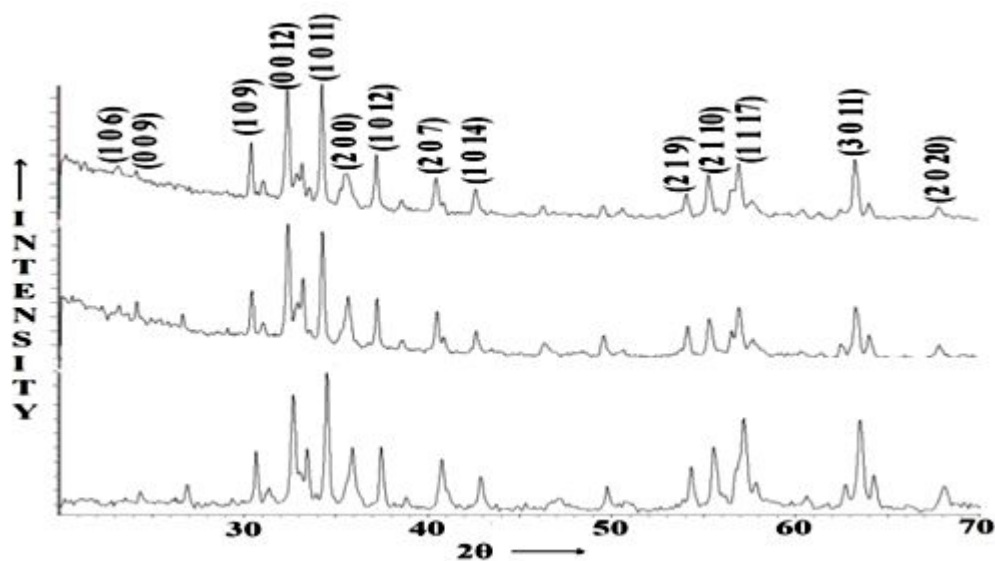
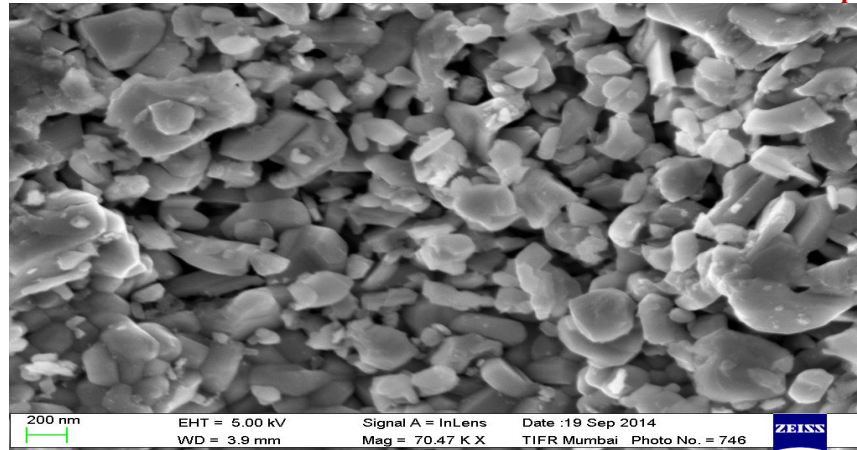
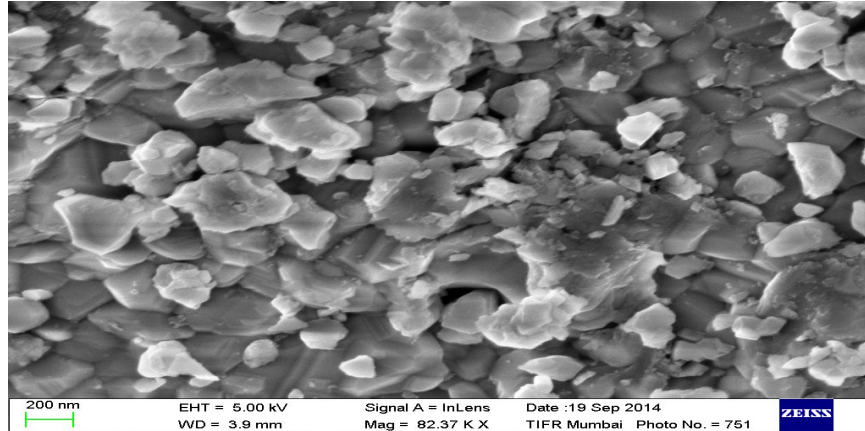


Figure 1: The XRD of Sr-Y hexaferrite compounds calcinated at different temp. for 4 and 6 hours.





*Figure 2(a): SrAl<sub>2</sub>Fe<sub>12</sub>O<sub>22</sub> calcinated at 1100<sup>o</sup>C for 6 Hrs*



*Figure 2(b): SrAl<sub>2</sub>Fe<sub>12</sub>O<sub>22</sub> calcinated at 1100<sup>o</sup>C for 4 Hrs*

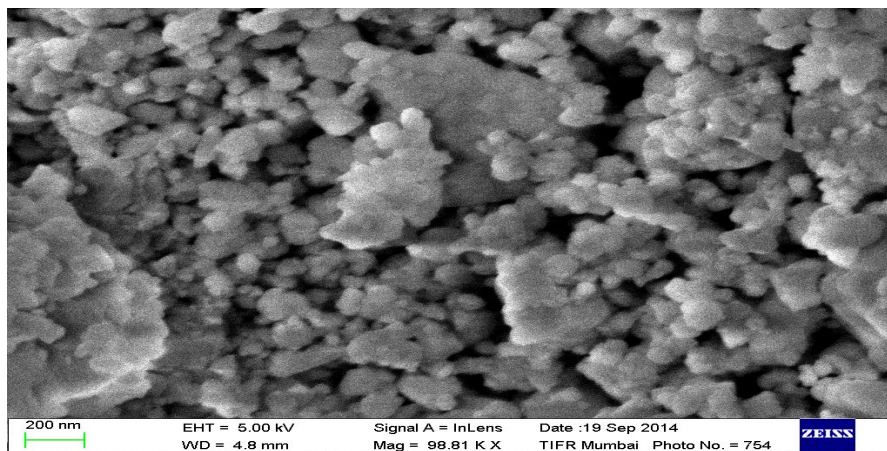


*Figure 2(c): SrAl<sub>2</sub>Fe<sub>12</sub>O<sub>22</sub> calcinated at 1000<sup>o</sup>C for 6 Hrs*

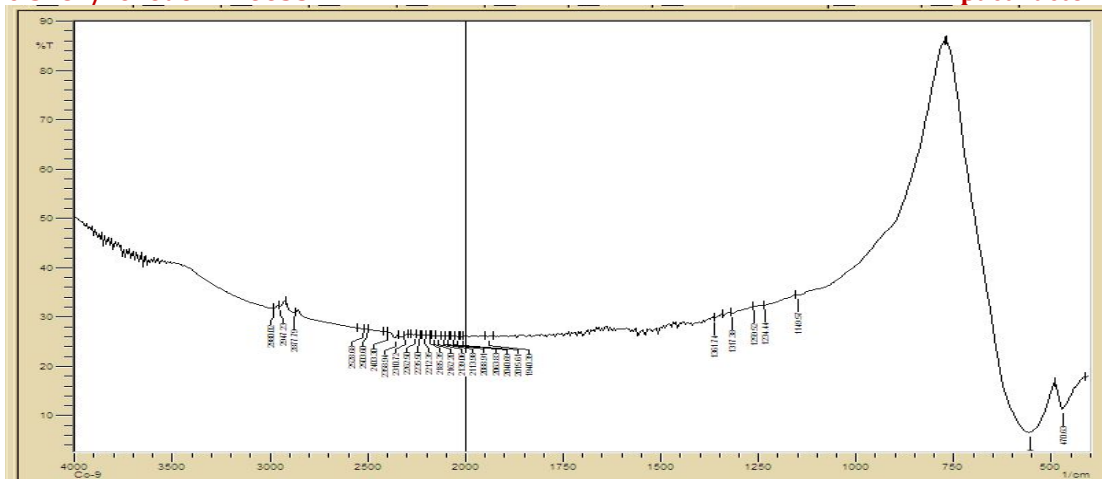


Figure 3(a): FTIR spectra of SrAl<sub>2</sub>Fe<sub>12</sub>O<sub>22</sub> calcinated at 1100°C for 6 Hrs.

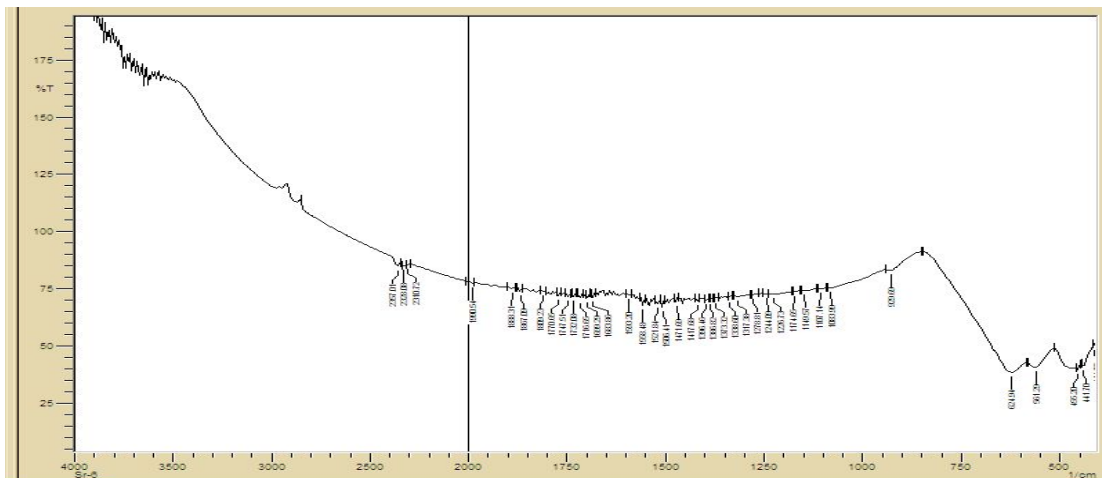


Figure 3(b): FTIR spectra of SrAl<sub>2</sub>Fe<sub>12</sub>O<sub>22</sub> calcinated at 1100°C for 4 Hrs.

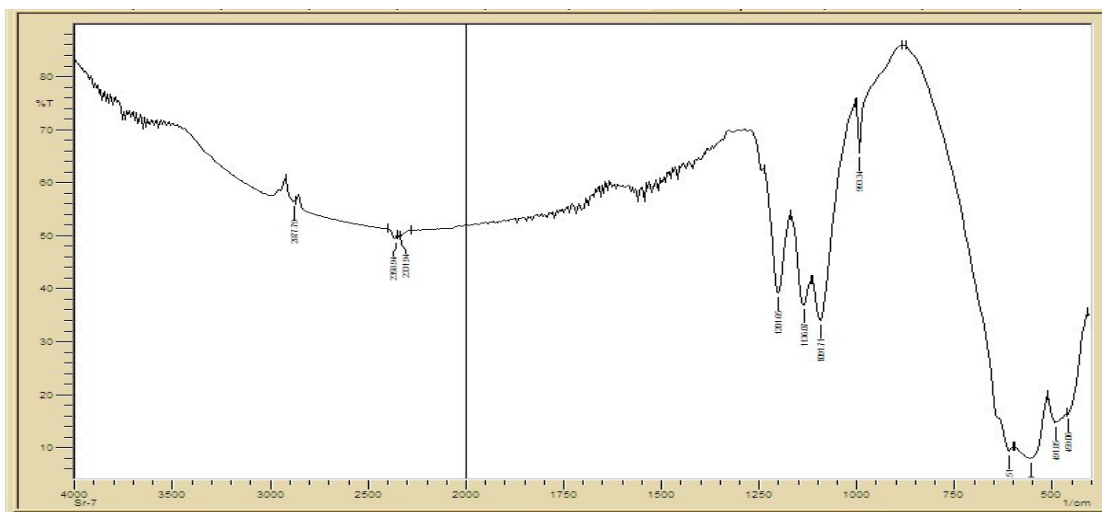


Figure 3(c): FTIR spectra of SrAl<sub>2</sub>Fe<sub>12</sub>O<sub>22</sub> calcinated at 1000°C for 6 Hrs.

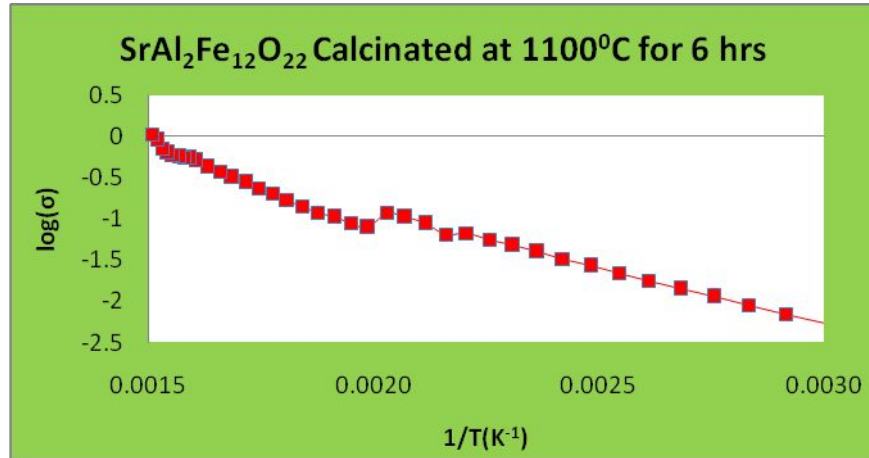


Figure 4(a): Plot of log (σ) versus 1/T of SrAl<sub>2</sub>Fe<sub>12</sub>O<sub>22</sub> calcinated at 1100<sup>0</sup>C for 6 Hrs.

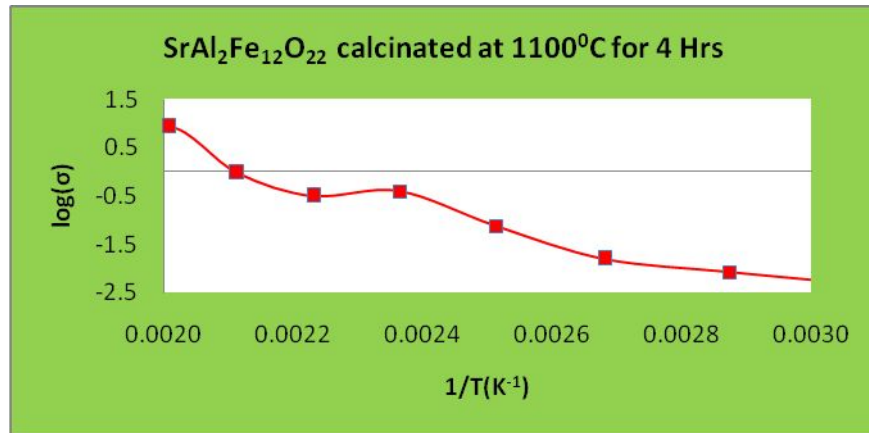


Figure 4(b): Plot of log (σ) versus 1/T of SrAl<sub>2</sub>Fe<sub>12</sub>O<sub>22</sub> calcinated at 1100<sup>0</sup>C for 4 Hrs.

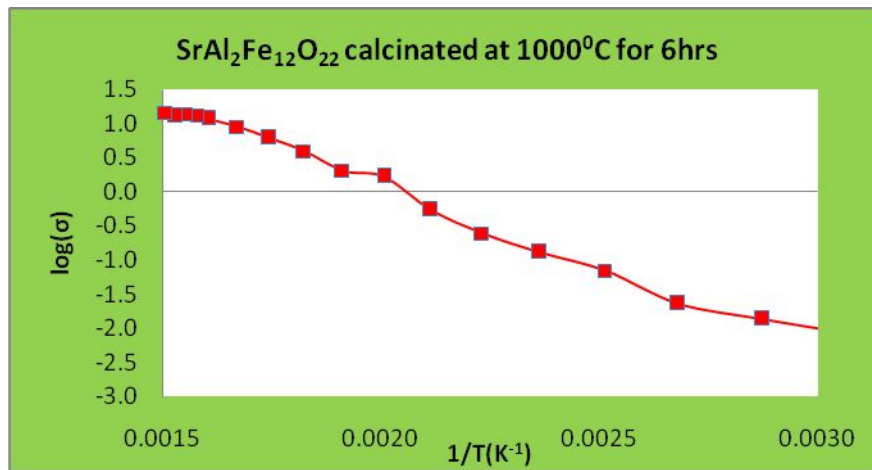


Figure 4(c): Plot of log (σ) versus 1/T of SrAl<sub>2</sub>Fe<sub>12</sub>O<sub>22</sub> calcinated at 1000<sup>0</sup>C for 6 Hrs.

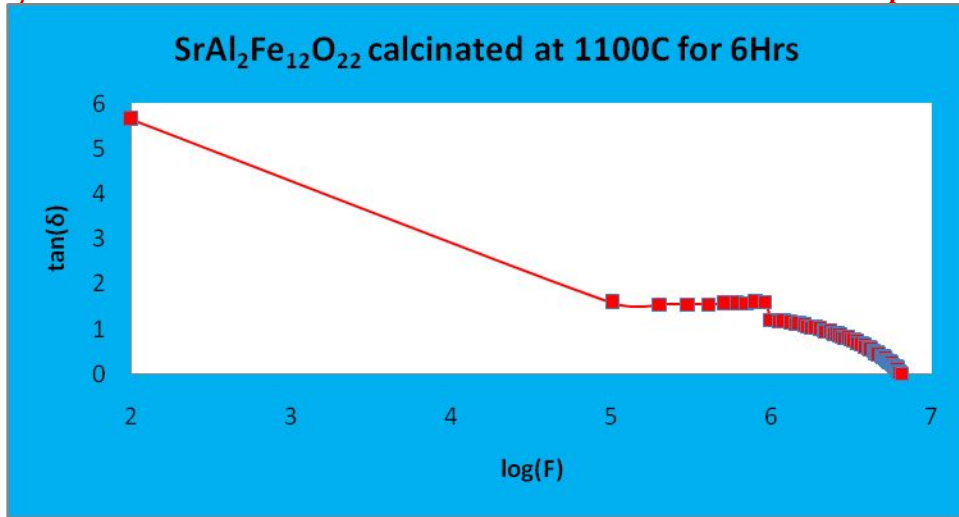


Figure 5(a): Plot of  $\tan(\delta)$  versus  $\log(F)$  of  $SrAl_2Fe_{12}O_{22}$  calcinated at  $1100^\circ C$  for 6 Hrs.

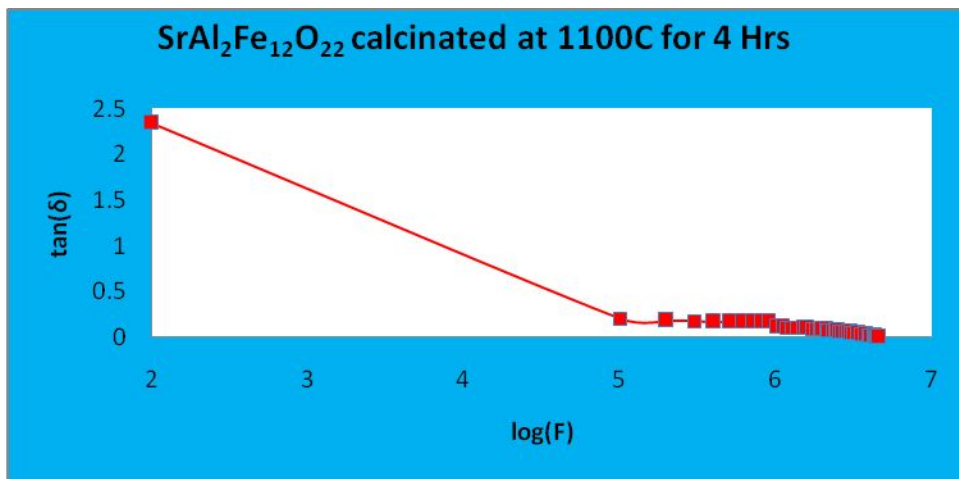


Figure 5(b): Plot of  $\tan(\delta)$  versus  $\log(F)$  of  $SrAl_2Fe_{12}O_{22}$  calcinated at  $1100^\circ C$  for 4 Hrs.

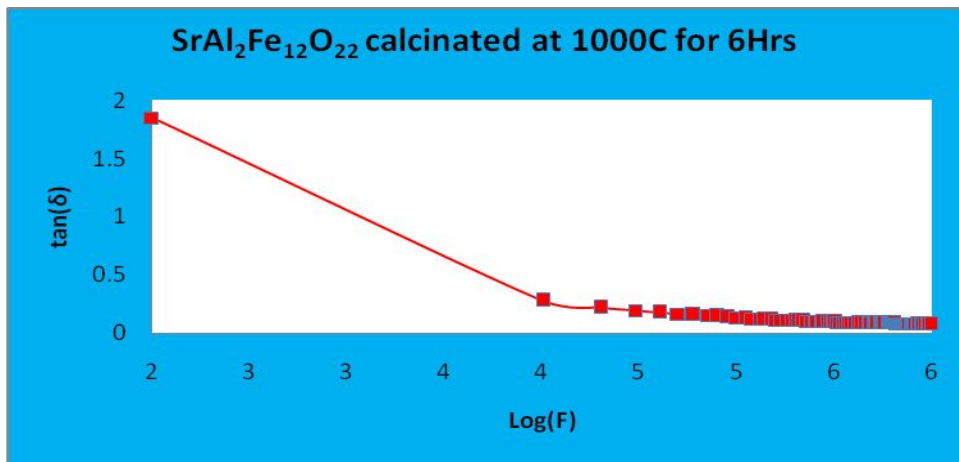


Figure 5(c): Plot of  $\tan(\delta)$  versus  $\log(F)$  of  $SrAl_2Fe_{12}O_{22}$  calcinated at  $1000^\circ C$  for 6 Hrs.

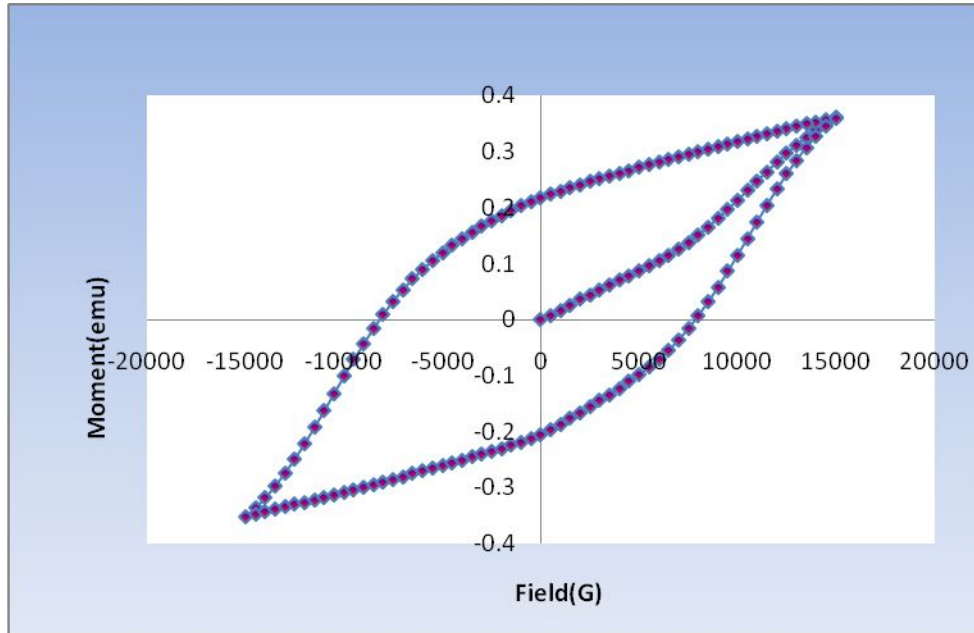


Figure 6(a): VSM of SrAl<sub>2</sub>Fe<sub>12</sub>O<sub>22</sub> compound calcinated at 1100°C for 6 Hrs.

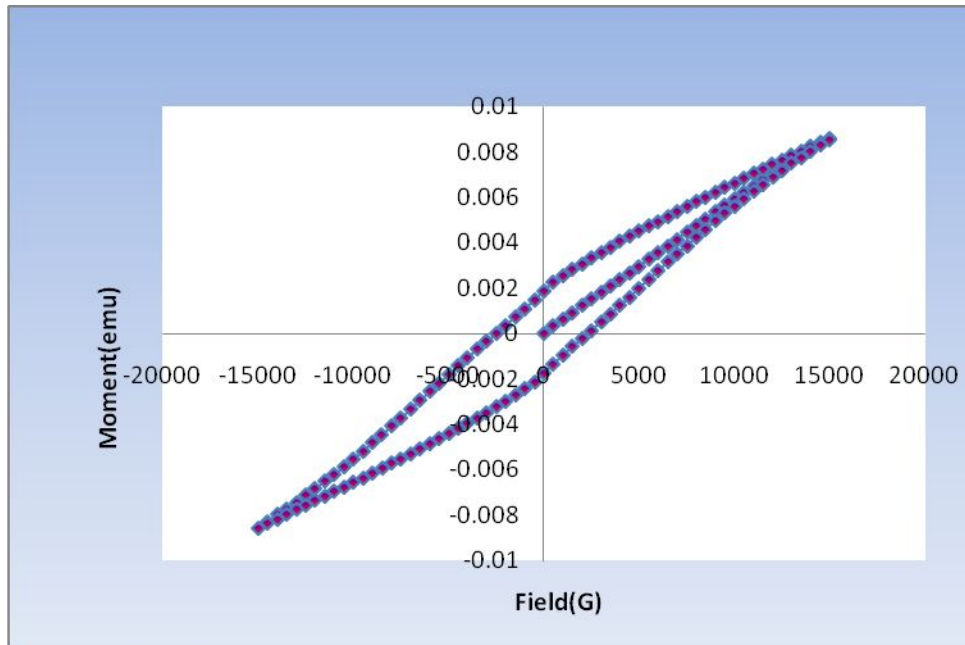


Figure 6(b): VSM of SrAl<sub>2</sub>Fe<sub>12</sub>O<sub>22</sub> compound calcinated at 1000°C for 6 Hrs.